

A Non-conforming Domain Decomposition Method for the Cardiac Potential Problem

M Pennacchio

Istituto di Analisi Numerica, CNR, Pavia, Italy

Abstract

A non-conforming non-overlapping domain decomposition based on the mortar method is applied to the cardiac potential problem. This problem is characterized by a narrow wavefront spreading through the myocardium. The numerical technique used allows adaptivity in the regions crossed by the wavefront thus increasing the accuracy of the computation. Numerical results illustrate how the method works and its efficiency if compared to the classical conforming Finite Element method.

1. Introduction

Numerical simulation of the heart's electrical activity is still a computationally intensive task due to the steep cardiac excitation wavefront spreading through the myocardium. Indeed, to accurately represent the narrow wavefront of the depolarization phase, very small space steps are required. Eikonal models allowed large scale simulations of the spread of excitation, with space steps of the order of 1 mm. If the transmembrane potential v is known, e.g. computed using eikonal approaches, then the extracellular potential u can be obtained solving an elliptic problem with source term depending on v . To approximate the extracellular field far from the wavefront the same spatial discretization used to solve the eikonal equation can be considered [1]. However, to accurately simulate the extracellular potential close to the wavefront very small space step has to be used. Adaptive approaches help to overcome the computational cost of the simulations and to resolve the steep gradients in the solution. For example in [2], to compute electrograms, an adaptive numerical technique applied to an integral representation of the extracellular potential was used.

In this work, a non-conforming non-overlapping domain decomposition, based on the mortar finite element method, is considered for an accurate computation of the extracellular potential in every regions, i.e. far and close to the wavefront. More specifically, by appropriate estimations of the transmembrane potential, we can determine in which part of the domain a finer grid is

necessary: typically the regions crossed by the wavefront. Then, this part is cut out as a new subdomain and a new finer grid can be constructed completely independent of the previous grid allowing a more accurate computation of the extracellular potential near the wavefront. Finally, using the mortar element method, the matching of different discretizations on adjacent subdomains can be weakly enforced [3, 4].

The numerical simulation results show the efficiency of this approach, if compared to the classical conforming Finite Element method, hence suggesting its use for more complex problems in electrocardiology.

2. Mathematical model

A well known macroscopic representation of the cardiac tissue is given by the *anisotropic bidomain*: the myocardium is seen as two interpenetrating anisotropic continua, intracellular (i) and extracellular (e), connected everywhere by the distributed cellular membrane [5]. The typical anisotropic myocardial fiber structure is modeled introducing the anisotropic conductivity tensors:

$$M_s = \sigma_t^s I + (\sigma_l^s - \sigma_t^s) \mathbf{a}\mathbf{a}^T \quad s = i, e \quad (1)$$

where $\mathbf{a} = \mathbf{a}(\mathbf{x})$ is the unit vector tangent to the cardiac fiber at a point $\mathbf{x} \in \Omega$ and σ_l^s , σ_t^s for $s = i, e$ are the conductivity coefficients, along and across fiber, in the (i) and (e) media, assumed constant with

$$\sigma_l^s > \sigma_t^s > 0 \quad \text{for } s = i, e. \quad (2)$$

If $v(\mathbf{x}, t)$ is known then, for each time instant t , the extracellular potential $u(\mathbf{x}, t)$ is solution of:

$$\begin{cases} \operatorname{div} M \nabla u(\mathbf{x}, t) = -\operatorname{div} M_i \nabla v(\mathbf{x}, t) & \text{in } \Omega \\ \mathbf{n}^T M \nabla u(\mathbf{x}, t) = -\mathbf{n}^T M_i \nabla v(\mathbf{x}, t) & \text{on } \Gamma = \partial\Omega \end{cases} \quad (3)$$

with $M = M_i + M_e$ and \mathbf{n} outward unit normal to Γ . Here, for simplicity but without loss of generality, we consider the case of H fully insulated even if the problem can be easily extended to the case of H in contact with extracardiac media such as blood or physiological fluid. In Problem (3) t is a parameter: if we want $u(\mathbf{x}, t)$ for a

sequence of time instants, t_1, t_2, \dots, t_n we have to solve (3) n times because the source term $-\text{div } M_i \nabla v(\mathbf{x}, t)$ depends on t .

The source term of (3) requires the knowledge of the transmembrane potential $v(\mathbf{x}, t)$ which was approximated using an eikonal approach. More specifically, the transmembrane potential is approximated by

$$v(\mathbf{x}, t) = \mathcal{A}(t - \varphi(\mathbf{x}))$$

with $\varphi(\mathbf{x})$ activation time, solution of the eikonal equation, and $\mathcal{A}(\tau)$ action potential upstroke. See [1] and the references therein for a detailed description of the eikonal model used.

3. Non-conforming approximation

The solution u of Problem (3) is characterized by a steeply rising layer identifying the cardiac wavefront. To increase the accuracy of the computation a domain decomposition method can be used. The regions crossed by the wavefront can be identified by an appropriate estimation of the transmembrane potential v . Hence, these regions are cut out as new subdomains and a new finer grid is constructed completely independent of the grid used far from the wavefront.

More specifically, let Ω be a bounded polygonal domain of \mathbb{R}^2 representing the cardiac tissue and let $\{\Omega_l\}_{l=1}^L$ be a partition of Ω into K non-overlapping subdomains Ω_l :

$$\Omega = \cup_{l=1}^L \Omega_l \quad \text{where} \quad \Omega_k \cap \Omega_l = \emptyset \quad \text{if} \quad k \neq l$$

assumed to be rectangular. For simplicity we assume a geometrically conforming domain decomposition, i.e. the intersection of the closure of two subdomains is either empty, a vertex, or an entire common edge of the two subdomains. Setting $\Gamma_{lk} = \partial\Omega_k \cap \partial\Omega_l$ then the so-called skeleton of the decomposition is

$$S = \cup \Gamma_{lk}.$$

We denote by $\gamma_l^{(i)}$ ($i = 1, \dots, 4$) the i -th side of the l -domain:

$$\partial\Omega_l = \cup_{i=1}^4 \gamma_l^{(i)}.$$

The Mortar Method is applied choosing a splitting of the skeleton S as the disjoint union of a certain number of subdomain sides $\gamma_l^{(i)}$, called *mortar* or *slave* sides. More precisely, we choose an index set $I \subset \{1, \dots, L\} \times \{1, \dots, 4\}$ such that

$$S = \bigcup_{(l,i) \in I} \gamma_l^{(i)}, \quad (l_1, i_1), (l_2, i_2) \in I \Rightarrow \gamma_{l_1}^{(i_1)} \cap \gamma_{l_2}^{(i_2)} = \emptyset$$

Finally $I^* \subset \{1, \dots, L\} \times \{1, \dots, 4\}$ will denote the index-set corresponding to *trace* sides or *master* sides which is defined as

$$I^* \cap I = \emptyset \quad \text{and} \quad S = \cup_{(l,i) \in I^*} \gamma_l^{(i)}.$$

Let now $X = \prod_{l=1}^L H^1(\Omega_l)$ and the following two composite bilinear forms $a, b: X \times X \rightarrow \mathbb{R}$:

$$a(u, w) := \sum_{l=1}^L \int_{\Omega_l} (\nabla u_l)^T M \nabla w_l \, dx$$

$$b(u, w) := \sum_{l=1}^L \int_{\Omega_l} (\nabla u_l)^T M_l \nabla w_l \, dx$$

The bilinear forms a_X and b_X are clearly not coercive on X , thus in order to obtain a well posed problem, proper subspaces of X has to be considered consisting of functions satisfying a suitable weak continuity constraint. More precisely, for any subspace $M \in L^2(S)$ let a *constrained* space $\mathcal{X}(M)$ be defined as follows:

$$\mathcal{X}(M) = \left\{ \phi \in X \mid \int_S [\phi] \lambda = 0, \quad \forall \lambda \in M \right\}$$

where $[\phi]$ denotes the jump of ϕ across the skeleton S . Then the following problem can be formulated:

Problem (P_M): Find $u_M \in \mathcal{X}(M)$ such that for all $\phi \in \mathcal{X}(M)$

$$a_X(u_M, \phi) = -b_X(v_M, \phi).$$

On each subdomains Ω_l independent meshes \mathcal{T}_l are considered so that typically nonconforming nodal points will occur on the boundaries between two adjacent subdomains. The space approximation is performed by introducing for each l a family \mathcal{V}_δ^l of finite dimensional subspaces of $H^1(\Omega_l) \cap C^0(\bar{\Omega}_l)$, depending on a parameter $\delta = \delta_l > 0$. Given a finite dimensional subspace $M_\delta \subset L^2(S)$, we will consider the following approximation of $H^1(\Omega)$:

$$\mathcal{X}_\delta = \left\{ \phi_\delta \in \prod_{l=1}^L \mathcal{V}_\delta^l, \quad \int_S [\phi_\delta] \lambda = 0, \quad \forall \lambda \in M_\delta \right\}$$

Thus the following discrete problem can be written:

Problem (P_δ): Find $u_\delta \in \mathcal{X}_\delta$ such that for all $\phi_\delta \in \mathcal{X}_\delta$

$$a(u_\delta, \phi_\delta) = -b(v_\delta, \phi_\delta) \quad (4)$$

3.1. Implementation

For each subdomain Ω_l we will denote by A^l and B^l the stiffness matrices relative to the discretization of the

operators $\mathcal{L}_M = -\text{div} M \nabla u$ and $\mathcal{L}_{M_i} = -\text{div} M_i \nabla u$ in \mathcal{V}_δ^l ; more precisely we have

$$A^l = \left\{ a_{ij} = \sum_{l=1}^L \int_{\Omega_l} (\nabla \phi_j)^T M \nabla \phi_i dx; j, i = 1, \dots, n_l \right\}$$

$$B^l = \left\{ b_{ij} = \sum_{l=1}^L \int_{\Omega_l} (\nabla \phi_j)^T M_i \nabla \phi_i dx; j, i = 1, \dots, n_l \right\}$$

An element u_δ of \mathcal{X}_δ has the form $u_\delta = (u_\delta^l)_{l=1, L}$ with $u_\delta^l = \sum_k u_k^l \Phi_k^l$; the coefficients (u_k^l) must satisfy the discrete equivalent of the jump constraint on the interface S .

The actual degrees of freedom, denoted by \mathbf{u}^M , are all the coefficients u_k^l corresponding to basis functions on Ω_l and those coefficients corresponding to a master side $(\gamma_l^{(i)}, (l, i) \notin I)$. The value of those coefficients u_k^l corresponding to basis functions "living" on mortar sides $(\gamma_l^{(i)}, (l, i) \in I)$ is uniquely determined by the remaining coefficients through the jump condition.

If we denote these last constrained coefficients by \mathbf{u}^S , we have that

$$\mathbf{u} = P \begin{pmatrix} \mathbf{u}^M \\ \mathbf{u}^S \end{pmatrix} \quad \text{and} \quad \mathbf{u}^S = C \mathbf{u}^M,$$

where P is a suitable permutation matrix and C is the matrix expressing the constraint.

It is well known that applying the stiffness matrix R_A , corresponding to problem (4) to the vector \mathbf{u}^M of degrees of freedom, can be rewritten as

$$R_A \mathbf{u}^M = [I \quad C^T] P^T \begin{pmatrix} A^1 & 0 & 0 \\ 0 & \ddots & 0 \\ 0 & 0 & A^L \end{pmatrix} P \begin{bmatrix} I \\ C \end{bmatrix} \mathbf{u}^M$$

with I identity matrix. The same structure can be obtained also for the source term, i.e. for the stiffness matrix R_B applied to \mathbf{v}^M ; therefore the algebraic formulation of problem (4) is given by:

$$R_A \mathbf{u}^M = -R_B \mathbf{v}^M. \quad (5)$$

The final matrix is symmetric and semidefinite and the system can be solved by an iterative method such as the Conjugate Gradient Method suitably preconditioned (see [6] for the preconditioning technique commonly used).

4. Results and conclusion

We now present some numerical results related to problem (3). More precisely we consider a domain $\Omega = [0, 1] \times [0, 1]$ cm with fibers parallel to a diagonal of

the square and the following conductivity coefficients: $\sigma_l^e = 2.5 \times 10^{-3}$, $\sigma_l^e = 1.25 \times 10^{-3}$, $\sigma_l^i = 2. \times 10^{-3}$ $\sigma_l^i = 4.16 \times 10^{-4}$ ($\Omega^{-1} \text{ cm}^{-1}$).

First example - We start by considering the computation of a potential map. Figure (1) refers to an extracellular potential map computed at 50 msec after stimulation and using an uniform grid, i.e. same space step far and close to the wavefront. Two different uniform grids have been considered: a coarse grid with a space step $dx = 3.33 \cdot 10^{-2}$ cm and a finer grid with $dx = 5.0 \cdot 10^{-3}$ cm. It appears clearly that the space step used on Fig.(1A) represents well the potential u far from the wavefront whereas numerical artifacts appears close to it. These artifacts disappear using a finer space step (see Fig.1B) but greatly increasing the number of points hence the computational cost.

The potential map without numerical artifacts can be obtained using the non-conforming approximation previously introduced (see Fig.(2B)). More specifically we used the space step of Fig.(1A) far from the wavefront and the same space step of Fig.(1B) close to it. The mesh considered in this case and the corresponding potential map are displayed in Fig.(2) A and B respectively.

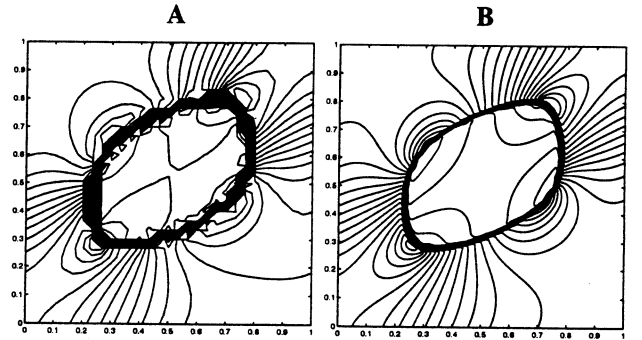


Figure 1. Conforming approximation: same space step dx far and close to the wavefront; $dx=3.33 \cdot 10^{-2}$ cm (A) and $dx=5.0 \cdot 10^{-3}$ cm (B).

Second example - We now consider the numerical simulation of an electrogram (EG). We fix a point in the domain Ω and we simulate the evolution of the extracellular potential u in this point. The EG obtained using the uniform coarser grid (see Fig. 3B) shows clearly the presence of spurious oscillations and peaks; these are mostly numerical artifacts since they disappear completely using the uniform finer grid (see Fig. 3C). Again, these numerical spurious oscillations can be avoided using the non conforming approximation, i.e. a mesh refinements only on a small region surrounding the observation point where the EG was computed. The mesh used and the EG obtained in this way are displayed in Fig.(4) A and B respectively.

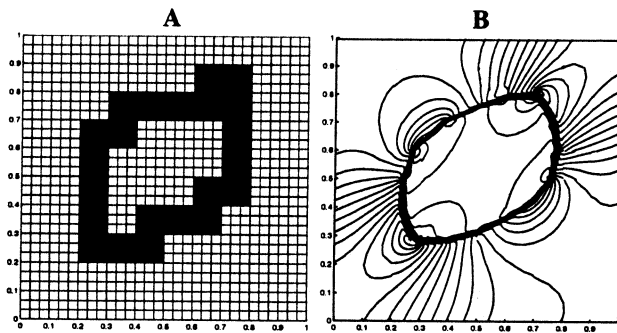


Figure 2. Non-conforming approximation: mesh used (A) and corresponding potential map (B). The mesh was refined only in the regions crossed by the wavefront.

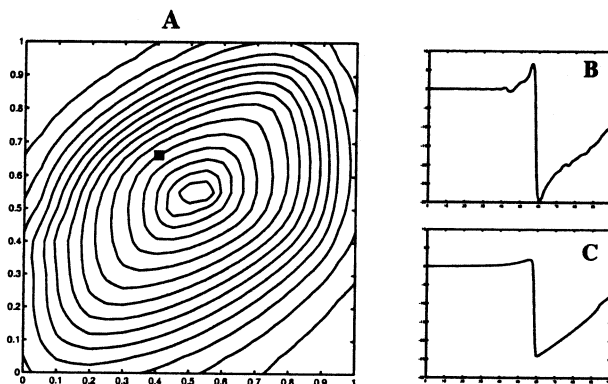


Figure 3. Conforming approximation. A: Isochrones (level lines of the activation time $\varphi(\mathbf{x})$) and position of the point where the EG is simulated. Corresponding EG computed using uniform meshes: space step $dx = 5.0 \cdot 10^{-2}$ cm (B) and $dx = 5.0 \cdot 10^{-3}$ cm (C).

In this paper a numerical method to compute the extracellular potential u is presented. The main aspect of the proposed method is the possibility to follow the cardiac excitation wavefront with a mesh totally independent of the mesh used far from it. This implies that a more accurate computation with a lower computational cost can be obtained. Indeed the numerical results showed the efficiency of this method, if compared with the conforming Finite Element method thus suggesting the possibility to extend it to more complex computational problem in electrocardiology.

Acknowledgments

The author thanks Dr. Silvia Bertoluzza for helpful suggestions and discussions.

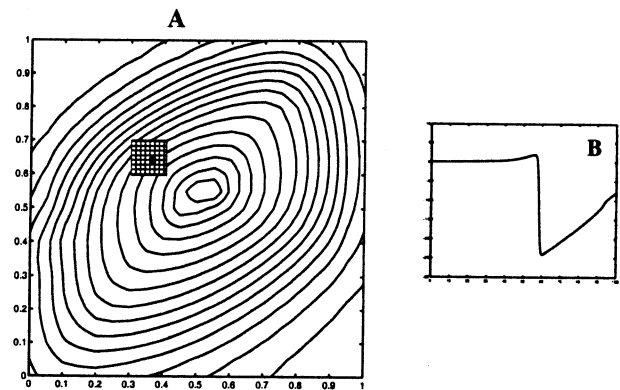


Figure 4. Non-conforming approximation. Isochrones and position of the point where the EG is computed (A). Corresponding EG (B). The mesh was refined only on a small region surrounding the observation point where the EG was simulated.

References

- [1] Colli Franzone P, Guerri L, Pennacchio M, Taccardi B. Spread of excitation in 3-D models of the anisotropic cardiac tissue. III: Effects of ventricular geometry and fiber structure on the potential distribution. *Math Biosci* 1998;151:51–98.
- [2] Colli Franzone P, Pennacchio M, Guerri L. Accurate computation of electrograms in the left ventricular wall. *Math Mod and Meth in Appl Sci* 2000;10(4):507–538.
- [3] Bernardi C, Maday Y, Patera AT. Domain decomposition by the mortar element method. In Kaper H, et al. (eds.), *Asymptotic and Numerical Method for Partial Differential Equations with Critical Parameters*. Dordrecht: Reidel, 1993; 269–286.
- [4] Bernardi C, Maday Y, Patera AT. A new nonconformnig approach to domain decomposition: The mortar element method. In Brezis H, Lions JL (eds.), *Nonlinear Partial Differential Equations and their Applications*, Collège de France Seminar, volume XI of Notes Math. Ser. 299. Boston: Pitman, 1994; 13–51.
- [5] Henriquez CS. Simulating the electrical behavior of cardiac tissue using the bidomain model. *Crit Rev Biomed Engr* 1993;21(1):1–77.
- [6] Wohlmuth BI. *Discretization Methods and Iterative Solvers Based On Domain Decomposition*, volume 17 of Lecture Notes in Computational Science and Engineering. Springer, 2001.

Address for correspondence:

Micol Pennacchio
Istituto di Analisi Numerica - CNR
via Ferrata, 1 / I-27100 Pavia / Italy
micol@ian.pv.cnr.i t